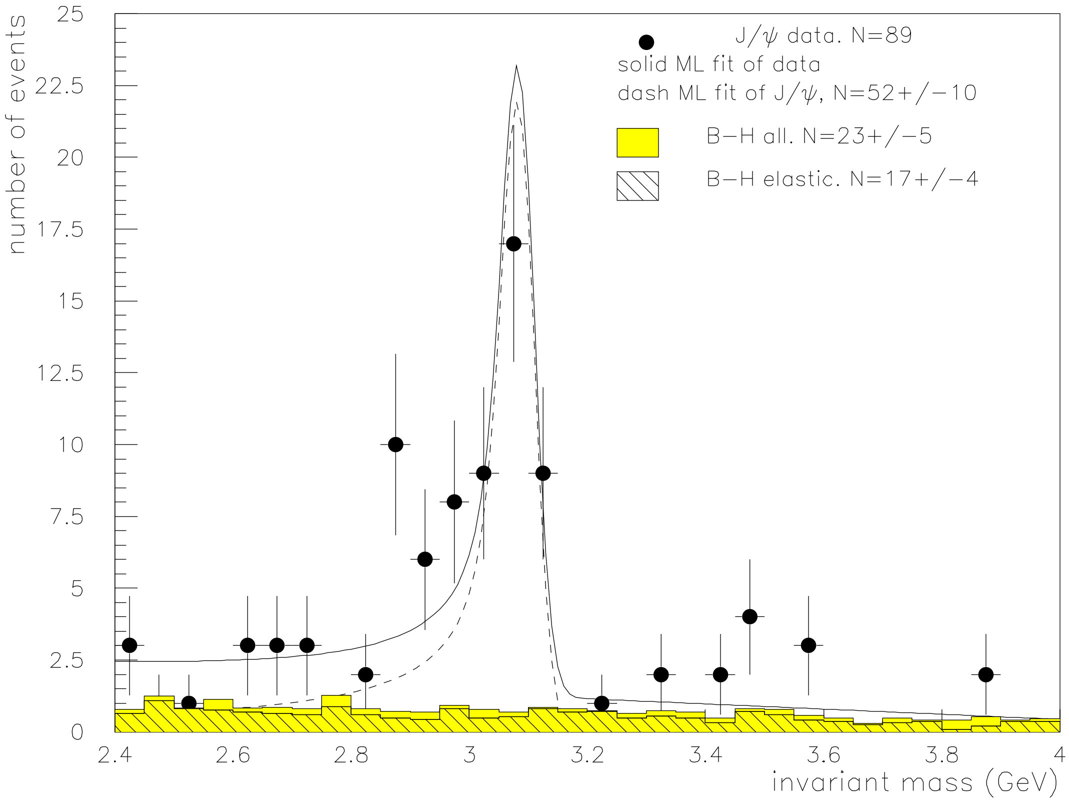

Figure 39: Invariant mass distribution of the elastic $J/\psi \to e^+e^-$ data($\bullet$) overlaid with Monte Carlo Bethe-Heitler background normalized to the data luminosity. The data is fitted by the maximum likelihood method with the function in Eq. (66). Dashed lines are fit curves of J/ψ(Gaussian and Bremsstrahlung tail). Solid lines include non-J/ψ(polynomials).

7.3 Resolution

Finite resolution in reconstructed kinematical variables can be a source of systematic errors. The interesting kinematic variables for elastic $J/\psi \to e^+e^-$ are $\sqrt{s_{\gamma p}}$, $t \approx p_t^2$ of J/ψ, and cosine of the lepton decay angle $\cos\theta_{\mathrm{decay}}$. Rapidity of J/ψ, y_{rap}, is approximately proportional to $-\log s_{\gamma p}$.

All these variables were reconstructed using the CTD measurements of e^+e^- tracks.

The MC events were first passed through the candidate selection procedure. Then the average deviation $(x_{\mathrm{MC}} - x_{\mathrm{REC}})$ and the r.m.s.(root mean square) of the deviation were calculated for each x_{REC} bin(iterated twice to get rid of long tails). The deviations are shown in Figure 40 and Figure 41. The r.m.s. of the deviations are shown as the vertical error bars.

7.4 Comparison of the data and Monte Carlo simulation

In this analysis, acceptance correction is based on the average acceptance $\langle\epsilon\rangle$ defined by

$$\langle\epsilon\rangle = \frac{\int \epsilon d\sigma_{ep}}{\int d\sigma_{ep}} \tag{69}$$

If the Monte Carlo generator reproduces the true distributions correctly, then the average acceptance can be determined simply by counting number of generated events and number of selected events. Figure 42 to Figure 46 show the comparisons of the J/ψ candidates and four Monte Carlo simulations in p_t^2 of J/ψ, y_{rap}, $\sqrt{s_{\gamma p}}$, $\theta_{J/\psi}$ and the decay cosine($\cos\theta_{\mathrm{decay}}$). Figure 49 to Figure 53 show the acceptance in these variables. Perhaps none of the MC agree with the real data in all regions of all variables. Apart from revealing disagreement between the true $d\sigma_{ep}/dx$ and $d\sigma_{ep}^{(MC)}/dx$ of the models, some errors in detector simulation of $\epsilon(x)$ may also be observable in these figures(x stands for one or a set of kinematic variables). For example, the angular distribution of e^+ and e^- should agree in any model and in the real data. However, Figure 47 and Figure 48 may indicate disagreement(it may or may not be accounted for by statistical fluctuations) in the real data between $\cos\theta_{e^+}$ and $\cos\theta_{e^-}$(in the laboratory frame). The two peak structure of the decay angular distribution in the real data (Figure 46) is not expected from any model. The disagreement between the real data and the MC in $\cos\theta_{\mathrm{decay}}$ perhaps reveals error in $\epsilon(x)$. It may also be due to statistical fluctuations and effects of pion contamination. The steep peak in y_{rap} of the real data may also be due to either pion contamination or systematic effects on $\epsilon(x)$.